Changes in the three-dimensional molecular structure of coal during methane adsorption induced swelling

Zhen Shen [a,*], Yu Liu [a,*], Junhuan Lei [a], Weijun Shen [b], Yuheng Wang [a], Cheng Xu [a], Jiaxun Gong [a]

[a] College of Geosciences and Surveying Engineering, China University of Mining and Technology (Beijing), Beijing 100083, China
[b] Key Laboratory for Mechanics in Fluid Solid Coupling Systems, Institute of Mechanics, Chinese Academy of Sciences, Beijing 100190, China

ABSTRACT

Methane (CH_4) adsorption-induced swelling is one of the critical factors controlling the permeability of coalbed methane (CBM). CH_4 adsorption alters the molecular structure of coal so as to induce coal swelling, and many uncertainties still exist in the process. In this study, the change in the molecular structures of different chemical structures by CH_4 adsorption was investigated using the Grand Canonical Monte Carlo method to simulate the alteration of bond lengths and bond angles during swelling. The results demonstrate that the alteration of chemical structure is more extensive than a chemical bond, which is the critical factor causing the swelling behavior. Owing to the complex molecular structure of coal, among the different types of chemical structures, the C-O-C (-O-) chemical structure showed the most significant change in bond angle, with the largest degree of change is 12.89%. Compared with other chemical structures, the C-C-C (aromatic -C-) chemical structures are more stable and the largest degree of change is 0.65%. For the different types of chemical bonds, the C-C chemical bonds showed the most significant change in bond lengths, with the largest degree of change is 2.94%. And the O-H chemical bond showed the smallest change, with the largest degree of change is 0.79%. Considering the structure evolution of coal, the C-O-C (-O-) chemical structure decreases with increasing maturity and changes to the greatest after the adsorption of methane. The aromatic structure increases and the degree of deformation decreases, which is consistent with the previous experimental values for swelling. These results reveal the details of different types of chemical group deformation, providing a molecular-level insight into adsorption swelling and permeability changes.

1. Introduction

Coalbed methane is a widely utilized natural gas and there has been significant interest in enhancing its production in recent years (Pan and Wood, 2015; Meng and Li, 2017; Wang et al., 2021). Methane is principally stored in the coal reservoir in an adsorbed state, and so changes in temperature and pressure will alter methane adsorption capacity. These changes can induce coal swelling and reduce the permeability of the coal reservoir (Pan and Connell, 2011; Moore, 2012; Liu et al., 2023; Wang et al., 2023). Although coal swelling due to methane adsorption has been extensively studied, the effects of different types of chemical structures in the coal macromolecules during swelling are still unclear (Levine et al., 1996; Palmer and Mansoori, 1998; Pan et al., 2010a, 2010b; Zhang et al., 2022). Since adsorption involves the interaction of forces between the coal macromolecular structure and the methane

molecules (Mosher et al., 2013; Liu et al., 2016; Lin et al., 2021), one of the keys to understanding the mechanisms of coal swelling at the molecular level is to elucidate the variations in bond lengths and bond angles of different types of chemical structures induced by gas adsorption (Fig. 1).

A combination of experimental and molecular simulations has been used to investigate the interactions between gas and coal that cause swelling. Moffat and Weale (1955) measured the swelling of different rank coals by methane adsorption. These experiments showed similar trends of coal swelling for different rank coals, with increasing pressures, coal swelling was large, and the swelling reached a peak at a pressure of 15 MPa. Following previous research, St. George and Barakat (2001) investigated the volumetric strain generated in coals induced by the adsorption of various gases at a pressure of 4 MPa. In this study, they found that the order of volume strain of coal induced by gas adsorption
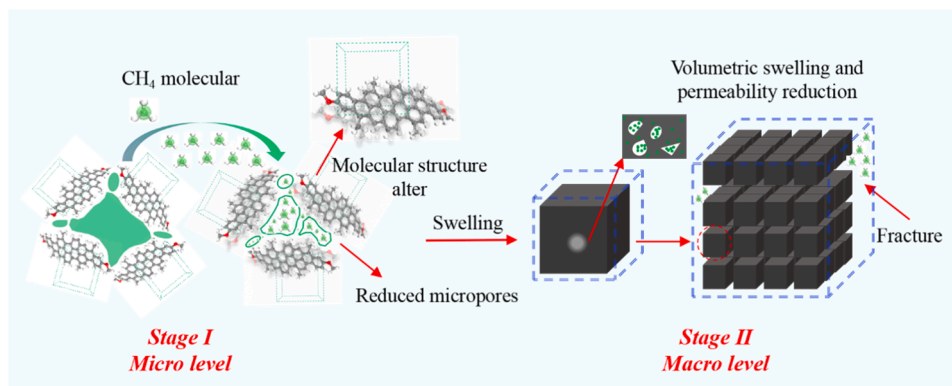
Fig. 1. Schematic diagram of CH$_4$ adsorption-induced swelling on coal matrix.

is CO$_2$ > CH$_4$ > N$_2$. Chikatamarla et al. (2004) interpreted that the amount of gas adsorbed and the volume strain is approximately linearly related for H$_2$S, CO$_2$, CH$_4$ and N$_2$ gas. Robertson and Christiansen (2005) measured the coal swelling induced by the adsorption of different types of gases on sub-bituminous and bituminous coal samples. Their results indicated the swelling of sub-bituminous coal induced by CO$_2$ adsorption was more than twice that of bituminous coal, although there are no differences in the amount of swelling caused by CH$_4$ and N$_2$ adsorption between sub-bituminous coal and bituminous coal. Day et al. (2008) showed that the deformation and swelling rate of Australian coals by CO$_2$ adsorption increases approximately linearly with increasing pressure until the pressure exceeds 10 MPa, after which the swelling does not change significantly. Using CH$_4$/CO$_2$ adsorption/desorption experiments, Majewska et al. (2010) showed that coal swelling rates depend on sorbate type and the coal rank. Wang et al. (2020) found from CO$_2$ adsorption experiments that coal swelling can be divided into three

parts: the slow stage, the rapid stage and the stable stage. Meng et al. (2022) performed CH$_4$ adsorption-induced coal swelling experiments and discovered that the degree of axial deformation is greater than that of the radial deformation in the initial stage of methane adsorption and that temperature has a greater effect on coal swelling than pressure.

There has also been an extensive amount of work in which the volumetric swelling of coal has been calculated by theoretical and molecular models (Wang et al., 2021). Based on the Langmuir equation, Levine et al. (1996) demonstrated that the theoretically calculated volume of coal swelling agreed well with the experimental volume. These results indicate that the swelling reduces the absolute permeability by volume expansion, and the coal matrix shrinkage might lead to increased fracture width. From an energy balance point of view, Pan and Connell (2007) calculated CH$_4$ and CO$_2$ adsorption using a theoretical model and discovered that CO$_2$ adsorption was more significant for coal swelling than CH$_4$ adsorption. Vandamme et al. (2010) utilized
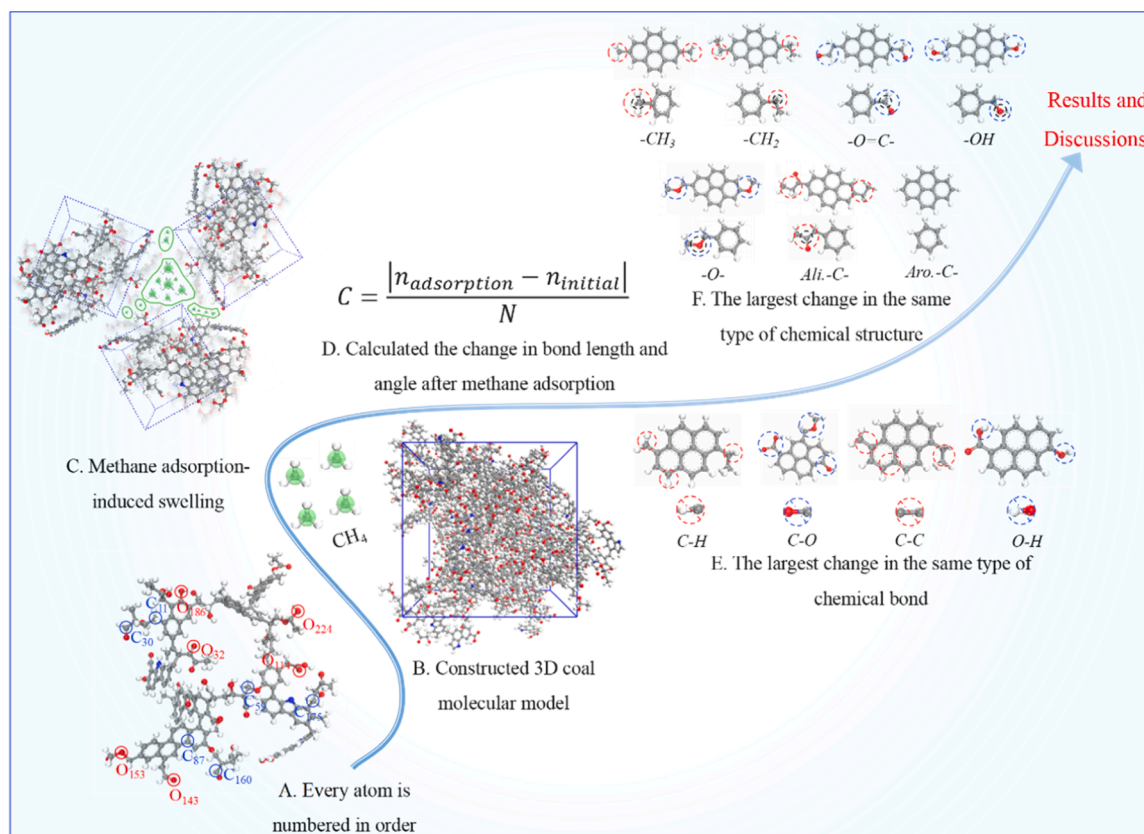

Fig. 2. The calculation process of CH$_4$ adsorption-induced swelling.

Table 1
The physical properties of rock (Shen and Meng, 2022).

Sample	$R_{o,m}$ (%)	Density (g/cm^3)	Proximate analysis			Coal composition			
			M_{ad} (%)	A_{ad} (%)	V_{ad} (%)	V (%)	I (%)	E (%)	M (%)
SH	2.91	1.47	1.92	8.62	6.25	94.30	0.47	0	5.23

Note: V- vitrinite, I- inertinite, E- exinite, M- mineral, M_{ad}- moisture A_{ad}- ash, V_{ad}- volatile matter.

molecular simulation methods to calculate the variations in the permeability of coal reservoir. Owing to the volume of coal swelling, the pores of the coal reservoirs would be closed, preventing the migration of gas. Using elastic rock mechanics and sorption parameters, a theoretical model was proposed by Liu and Harpalani (2013) to calculate the coal swelling or shrinkage during gas adsorption or desorption. Zhang et al. (2015) calculated the volume of coal swelling due to competitive adsorption at different burial depths by Grand Canonical Monte Carlo (GCMC) simulations and the volumetric strain increase with increasing CO_2 bulk mole fraction. Zhang et al. (2020) demonstrated that the degree of coal swelling and shrinkage was influenced by the pore size during CO_2 adsorption and desorption. Owing to the competitive adsorption of binary gas mixtures, Chen et al. (2021) used molecular simulations to study coal swelling. They found that the swelling ratio of the coal volume increased with the increasing CO_2 bulk mole fraction in the adsorption of $CH_4 + CO_2$, while the swelling ratio of the coal volume decreased with the increasing N_2 molar fraction in $CH_4 + N_4$ adsorption.

As mentioned above, there are numerous experiments and theoretical models that investigate the volume of coal swelling caused by gas adsorption. However, the changes in the molecular conformation of different types of chemical structures during adsorption-induced coal swelling have rarely been studied, as shown in Fig. 2. In this study, the adsorption behavior of methane and the deformation characteristics of different types of chemical bonds and chemical structures will be investigated to elucidate the mechanisms of the coal swelling at the molecular level and to enhance the understanding of adsorption-induced swelling processes (Fig. 2).

2. Molecular simulation methods

2.1. Coal sample

Coal samples were obtained from the Sihe (SH) Coal Mine, the northern Qinshui Basin, China. These coal samples were broken to 60–80 mesh and put into a vacuum drying oven to remove moisture at 378.15 K for 24 h. Subsequently, the experiment was conducted to analyze the physical properties of rock (Table 1). Simultaneously, to study the behavior of methane adsorption swelling at the molecular level, a combination of methods, including ^{13}C NMR, XPS and FTIR experiments (Fig. 3), were used to construct the molecular structure of coal. Owing to we have already completed relevant experiments in our previous research results (Shen and Meng, 2022), we cited our previous work to construct a coal molecular model and explore the behavior of methane adsorption swelling.

2.2. Building the molecular structure of coal

In this study, the molecular structure model of coal developed by Shen and Meng (2022) was employed. The molecular structure model was used to represent high-rank coal with a composition of $C_{184}H_{163}N_3O_{37}$ for the simulation of methane adsorption-induced coal swelling. The 2D chemical molecular structure of the anthracite coal was constructed using Materials Studio (MS) software, as shown in Fig. 3, where the carbon, hydrogen, nitrogen and oxygen atoms are expressed by grey, white, blue and red colors. The sub-figures A – I, marked with arrows, represent the structural units that are shown in the center box. In addition, every atom was numbered in order by the MS software (Liu

et al., 2021).

The 3D spatial structure model of anthracite coal is based on the optimized 2D chemical molecular structure and experimental results. The description of the molecular model can be found in our previous work (Shen and Meng, 2022). This model was applied to simulate the effects of methane adsorption in the anthracite coal molecular on the evolution of bond lengths and bond angles of different types of chemical structures, as shown in Fig. 3. From Fig. 3, there are 14 optimized anthracite coal molecular structure are put into a unit cell, which is represented by different colors. And the Van der Waals forces exist between the methane molecules adsorbed in the coal molecular structure and the chemical bond types, and the effects of these forces can affect the different types of chemical structures in the coal molecular structure. In addition, changes in temperature and pressure change the amount of methane adsorbed in the coal molecular structure, which also results in the alteration of the bond lengths and bond angles between the chemical structures and the coal macromolecular structure. The simulation results were used to calculate the degree of deformation of bond lengths and bond angles of different types of chemical structures in the structure of anthracite coal macromolecules after methane adsorption.

2.3. Molecular simulation methods

From Fig. 3, the C, H, O, and N atoms were labeled with numbers and the C-H, C-O, C-C, and O-H chemical bonds and the H-C-H (methyl and methylene), O-C-H (carbonyl), H-O-C (hydroxyl), -O- (ether), -C- (aliphatic -C- and aromatic -C-) chemical structures were measured in the 3D molecular structure of coal. The Sorption Module of the Grand Canonical Monte Carlo (GCMC) method to calculate the adsorption behavior of methane by molecular simulation (Liu et al., 2016; Gotzias et al., 2013). The adsorption of methane molecules is due to the interaction of Van der Waals forces between the molecules in the micropores and the functional bond groups in the molecular structure of coal (Mosher et al., 2013). The Condensed-phased Optimized Molecular Potentials for Atomistic Simulation Studies (COMPASS) field was selected (Hu et al., 2010), and the van der Waals forces interactions were calculated using the Lennard-Jones 9–6 equation (Sun, 1998; Liu et al., 2018a, 2018b; Shen and Meng, 2022). In the calculation, the Ultra-fine quality was selected to explore the characteristics of methane adsorption equilibrium in the Sorption module. Subsequently, the results of the simulations were used to calculate the initial values and the values of the absolute alter in bond length and bond angle between coal 3D-molecule after methane adsorption under different conditions.

3. Results

3.1. Simulation of methane adsorption

Fig. 4 describes the methane adsorption capacity under different temperature and pressure conditions. As the pressure increases, the adsorption of methane is initially rapid, but the rate decreases with increasing pressure. For example, as pressure enhances from 1 MPa to 5 MPa at the temperature of 20 ℃, the adsorption amount of methane increases from 22.58 cm^3/g to 32.23 cm^3/g, which is an increase of 42.71%. As pressure enhances from 5 MPa to 10 MPa, the adsorption amount of methane increases from 32.23 cm^3/g to 35.71 cm^3/g, which is an increase of 10.78%. In contrast, as the temperature rises, the
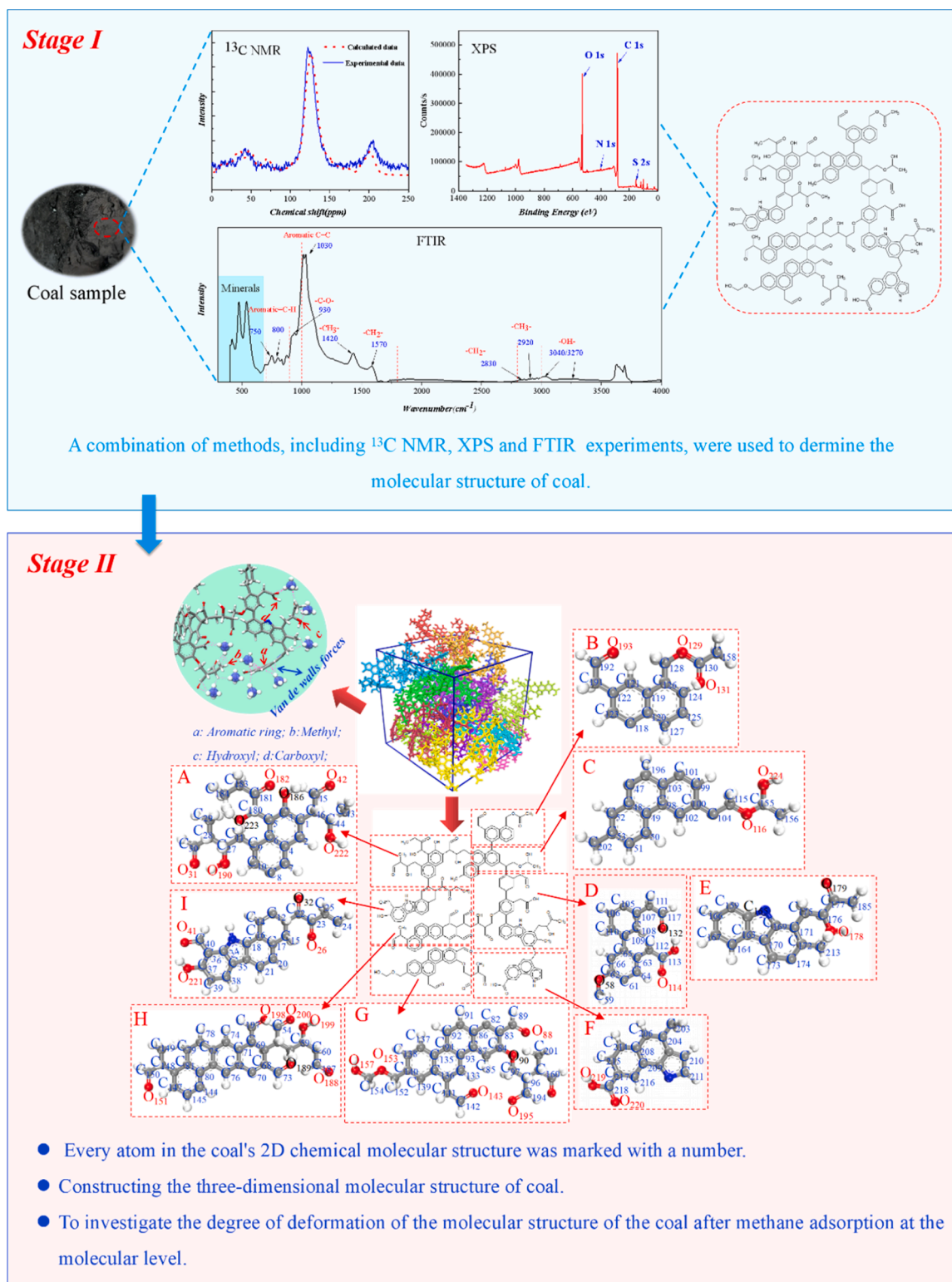
Fig. 3. Construction process and spatial distribution characteristics of the molecular structure of anthracite coal. (The coal molecule is reconstructed from our previous work (Shen and Meng, 2022).)

adsorption capacity of methane gradually weakens. For example, at a pressure of 10 MPa, as the temperature rises from 20 °C to 60 °C, the adsorption amount decreases from 35.71 cm^3/g to 29.09 cm^3/g, which is a decrease of 18.53%.

3.2. The Effect of temperature on the deformation degree of coal molecular

At a pressure of 10 MPa, as the temperature rises from 20 °C to 60 °C, the simulations of methane adsorption on the coal 3D-molecule were done, and the bond lengths and bond angles were calculated from these
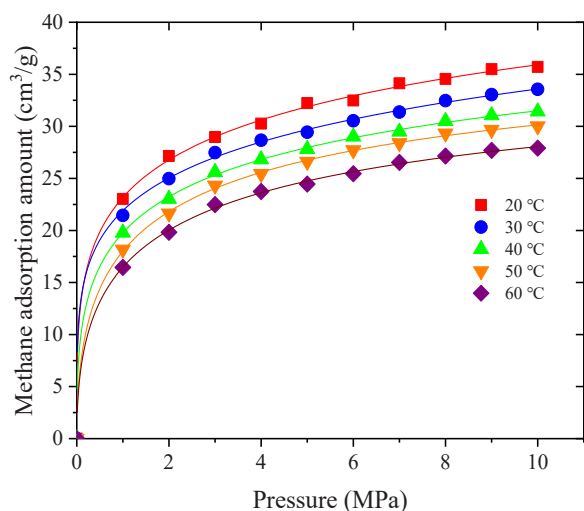
Fig. 4. Adsorption capacity of methane at different temperatures.

simulation results. Owing to the large amount of data in this study, the same type of chemical bonds and chemical structures with the largest deformation contribution were counted for every single coal macromolecular structure. The deformation contribution can be expressed by Eq. (1):

$$C = \frac{|n_{ads} - n_{ini}|}{N} \tag{1}$$

Where n_{ini} is the initial value of the functional bond group in the coal macromolecule; n_{ads} is the value of the functional bond group after methane adsorption; N is the total value of the functional bond group deformation after methane adsorption; C is the deformation contribution.

Fig. 5 shows the contribution of chemical bonds to deformation in the molecular structure of coal (the numbering of the C, H, O, and N atoms (Fig. 3). At a pressure of 10 MPa, as the temperature increases from 0 ℃ to 60 ℃, the deformation contribution of C-H, C-O, C-C, and O-H chemical bonds in the coal 3D-molecule is 18.86%, 19.35%, 55.66%, and 6.14%, respectively. And the deformation degree of C-H, C-O, C-C, and O-H chemical bonds in the coal 3D-molecule is 0.08%– 1.04%, 0.08%– 0.92%, 0.17%– 2.94%, and 0.05%– 0.63%, respectively (Table 2). The results reveal that the C-C chemical bonds are most affected by methane adsorption, while the O-H chemical bonds are less affected. It also illustrates that the C-C chemical bonds are more

sensitive to methane adsorption than other chemical bonds and their bond lengths are more likely to change.

Methane adsorption will also result in the deformation of chemical structures. Fig. 6 shows the contribution of bond angles to the deformation in different types of chemical structures. The deformation contribution of H-C-H (-CH₃), H-C-H (-CH₂), O-C-H (-O═C-), H-O-C (-OH), C-O-C (-O-), C-C-C (aliphatic -C-) and C-C-C (aromatic -C-) chemical structures in the coal 3D-molecule is 5.42%, 12.27%, 4.26%, 10.30%, 35.94%, 28.00% and 3.72%, respectively. Simultaneously, the deformation degree of H-C-H (-CH₃), H-C-H (-CH₂), O-C-H (-O═C-), H-O-C (-OH), C-O-C (-O-), C-C-C (aliphatic -C-) and C-C-C (aromatic -C-) chemical structures in the coal 3D-molecule is 0.26%– 3.38%, 0.10%– 3.01%, 0.02%– 1.03%, 0.19%– 1.88%, 0.18%– 11.39%, 0.10%– 8.04% and 0.12%– 0.79% respectively (Table 2). The results reveal that the C-O-C (-O-) and C-C-C (aliphatic -C-) chemical structures are more altered by methane adsorption than other chemical structures. While the C-C-C (aromatic -C-) chemical structures are less altered. Since there are only two carboxyl chemical structures (-COOH) in the coal 3D-molecule, they aren't described in the results.

3.3. The Effect of pressure on the deformation degree of coal molecular

In order to investigate the effect of pressure on swelling, the chemical bonds and chemical structures in the coal 3D-molecule were simulated. Similar to the results of the temperature variation study, the deformation contribution of the chemical bond and chemical structures are shown in Fig. 5 and Fig. 6.

Fig. 5 shows the contribution of chemical bonds to deformation in

Table 2
The range of deformation of chemical bonds and chemical structures in the coal 3D-molecule at the temperature ranging from 0° to 60°.

Temperature (from 0° to 60°)			
Chemical Bond	Deformation Degree (%)	Chemical Structure	Deformation Degree (%)
C-H	0.08–1.04	-CH₃	0.26–3.38
		-CH₂	0.10–3.01
C-O	0.08–0.92	-O═C-	0.02–1.03
		-OH	0.19–1.88
C-C	0.17–2.94	-O-	0.18–11.39
		Ali.-C-	0.10–8.04
O-H	0.05–0.63	Aro.-C-	0.12–0.79

(Note: the Ali.-C- represents Aliphatic C; the Aro.-C- represents Aromatic C)
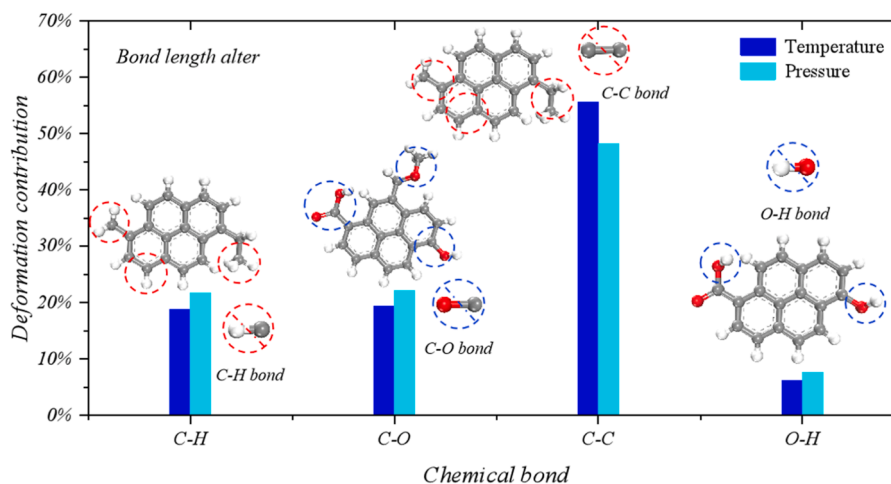

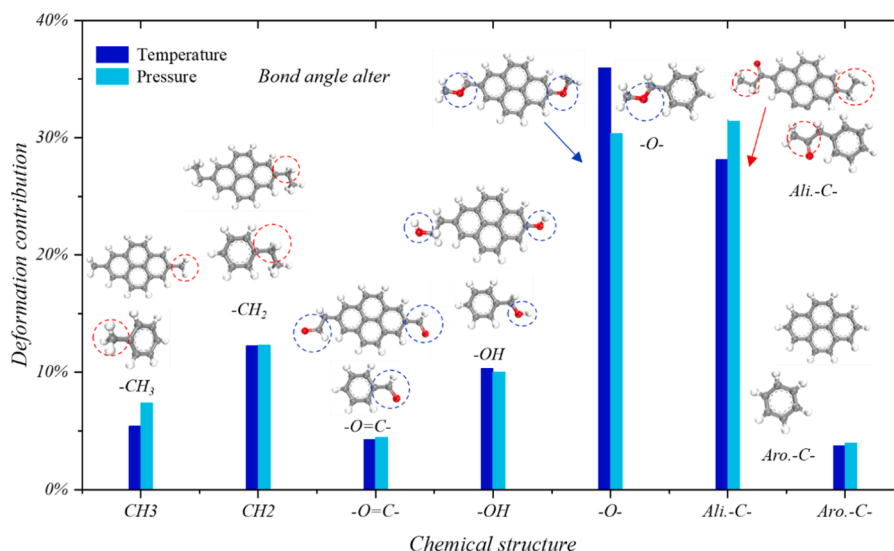**Fig. 5.** Contribution of different chemical bonds to deformation.

Fig. 6. Contribution of different chemical structures to deformation.

Table 3
The range of deformation of chemical bonds and chemical structures in the coal 3D-molecule at the pressure ranging from 0 MPa to 10 MPa.

Pressure (from 0 MPa to10 MPa)			
Chemical Bond	Deformation (%)	Chemical Structure	Deformation (%)
C-H	0.03–1.09	CH_3	0.01–3.38
		CH_2	0.07–3.71
C-O	0.08–0.97	-O=C-	0.07–1.13
		OH	0.18–2.89
C-C	0.01–1.77	-O-	0.39–12.89
		Ali.-C-	0.51–8.01
O-H	0.04–0.65	Aro.-C-	0.11–0.77

the molecular structure of coal. At a temperature of 20 ℃, as the pressure increases from 0 MPa to 10 MPa, the deformation contribution of C-H, C-O, C-C, and O-H chemical bonds in the coal 3D-molecule is 21.72%,

22.41%, 48.22%, and 7.65%, respectively. And the deformation degree of C-H, C-O, C-C, and O-H chemical bonds in the coal 3D-molecule is 0.03%– 1.09%, 0.08%– 0.97%, 0.01%– 1.77%, and 0.04%– 0.65% respectively (Table 3). The results illustrate that the C-C chemical bonds are more sensitive to methane adsorption, while the O-H chemical bonds are less affected.

Fig. 6 shows the contribution of bond angles to deformation in different types of chemical structures. The deformation contribution of H-C-H (-CH_3), H-C-H (-CH_2), O-C-H (-O=C-), H-O-C (-OH), C-O-C (-O-), C-C-C (aliphatic -C-), C-C-C (aromatic -C-) chemical structures in the coal 3D-molecule is 7.39%, 12.31%, 4.46%, 10.00%, 30.32%, 31.54% and 3.97%, respectively. Simultaneously, the deformation degree of H-C-H (-CH_3), H-C-H (-CH_2), O-C-H (-O=C-), H-O-C (-OH), C-C-C (aliphatic -C-) and C-C-C (aromatic -C-) chemical structures in the coal 3D-molecule is 0.01%– 3.38%, 0.07%– 3.71%, 0.07%– 1.13%, 0.18%– 2.89%, 0.39%– 12.89%, 0.51%– 8.01% and 0.11%– 0.77% respectively (Table 3). In the same way, the C-O-C (-O-) and C-C-C
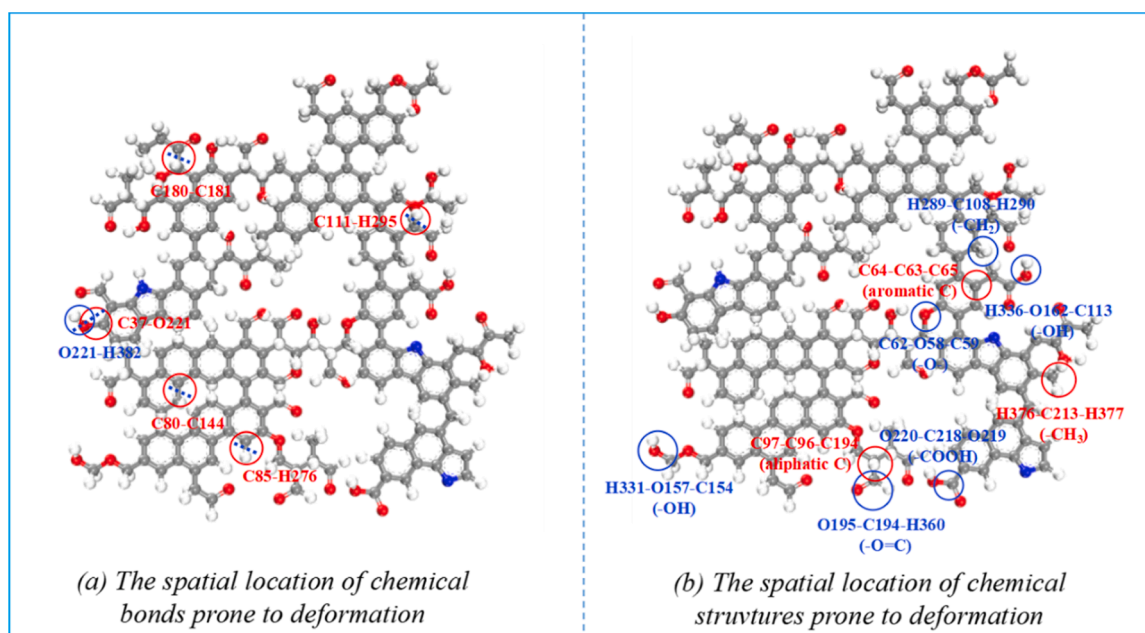

Fig. 7. The spatial distribution characteristic of chemical bonds and chemical structure prone to deformation.
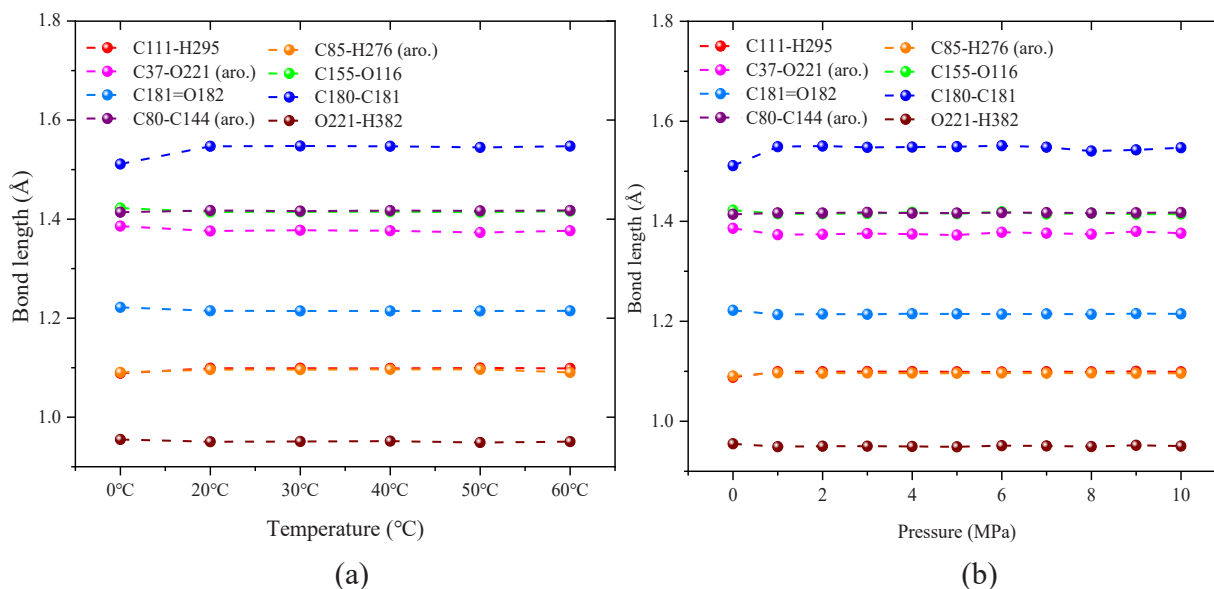
Fig. 8. Variation values of bond lengths for different types of chemical bonds. (a. Changes in bond length at different temperatures; b. Changes in bond length at different pressures.).

(aliphatic -C-) chemical structures are more facilely altered by methane adsorption than other chemical structures. The C-C-C (aromatic -C-) chemical structures are less altered.

4. Discussions

4.1. Temperature effect on chemical bonds and chemical structures

In simulations with temperature ranges of 0 ℃− 60 ℃, the absolute values of bond length changes are greatest in the C111-H295, C37-O221, C180-C181 and O221-H382 chemical bonds before and after methane adsorption, their spatial position in the coal 3D-molecule is shown in Fig. 7. Note that there are a few chemical bonds on aromatic rings that are susceptible to change, including the C85-H276, C37-O221, and C80-C144 chemical bonds. In addition, the more sensitive to deformation of C-H, C-O and C-C chemical bond types on the aromatic ring are 1:13, 1:6 and 1:17 than the aliphatic structure in the coal 3D-molecule. The results indicate that with temperature variations the C-C, C-O, and C-H chemical bond types connected to aromatic rings are less affected by methane adsorption (and less easily deformed) than the C-C, C-O, and C-H bond types in aliphatic structures. This difference suggests that chemical bonds on the aromatic ring are more stable than on aliphatic structures and that the aromatic ring is less prone to deformation.

The simulations indicate that the bond angles of different types of chemical structures are altered to a larger extent by methane adsorption than the bond lengths. The largest deformations occur in the chemical structures H376-C213-H377 (-CH₃), H289-C108-H290 (-CH₂), O195-C194-H360 (-O=C-), O220-C218-O219 (-COOH), H336-O162-C113 (-OH), C62-O58-C59 (-O-), C97-C96-C194 (aliphatic -C-) and C64-C63-C65 (aromatic -C-) during the adsorption of methane in the coal 3D-molecule. These are the most likely to undergo deformation leading to swelling, as shown in Fig. 7.

The preceding discussion indicates that the bond lengths and bond angles of the aliphatic side chains in the coal macromolecular structure are sensitive to alteration by interaction with methane molecules. The simulations also demonstrate that aliphatic side chains are susceptible to being cracked from the coal macromolecular structure at specific locations. However, aromatic structures are relatively and are not easily deformed with increasing temperature. In addition, the positions at which the greatest deformations occur may change with increasing temperature. Because of the interaction forces between molecules,

different types of chemical structures are close to the methane molecule in the coal 3D-molecule, then, they will deform more severely.

4.2. Pressure effect on chemical bonds and chemical structures

The pressure of the adsorbed methane is an important factor in determining the extent of alteration of the bond lengths and bond angles and the increase in methane adsorption capacity (Fig. 4). In general, increases in pressure result in a greater degree of deformation. The simulation results indicate that the absolute values of the changes in bond lengths are largest in C111-H295, C37-O221, C180-C181 and O221-H382 chemical bonds before and after methane adsorption, as shown in Fig. 7. There are only a limited number of chemical bonds connected to aromatic rings that are sensitive to change, including as C85-H276, C37-O221, and C80-C144 chemical bonds. The more sensitive to deformation of C-H, C-O and C-C chemical bond types on the aromatic ring are 1:9, 1:6 and 1:27 than the aliphatic structure in the coal 3D-molecule. Simultaneously, the absolute values of the bond angles also change with increasing pressure. The largest deformations occur in chemical structures H376-C213-H377 (-CH₃), H289-C108-H290 (-CH₂), O195-C194-H360 (-O=C-), O220-C218-O219 (-COOH), H331-O157-C154 (-OH), C62-O58-C59 (-O-), C97-C96-C194 (aliphatic -C-) and C64-C63-C65 (aromatic -C-) during the adsorption of methane in the coal macromolecular structure, as shown in Fig. 7. The simulation results also show that the spatial locations of the most extensive bond length and bond angle deformations for pressure-induced changes and temperature-induced changes are similar. The intermolecular forces will change both bond lengths and bond angles by increasing or decreasing the number of methane molecules interacting with the coal molecular structure. This effect demonstrates that, because of their conformations, some chemical structures in the coal matrix are more predisposed to interact with the methane sorbate. These structures will generally be the most susceptible to alteration by external forces (e.g., cracking).

4.3. Variation range of chemical bonds and chemical structures

Based on the values of C-H, C-O, C-C and O-H chemical bond lengths (1.08–1.12 Å, 1.20–1.45 Å, 1.34–1.62 Å and 0.95–0.98 Å), and the values of H-C-H (-CH₃), H-C-H (-CH₂), O-C-H (-O=C-), O=C-O (-COOH), H-O-C (-OH), C-O-C (-O-), C-C-C (aliphatic -C-) and C-C-C (aromatic -C-) chemical structure angles (104.57°−110.82°,
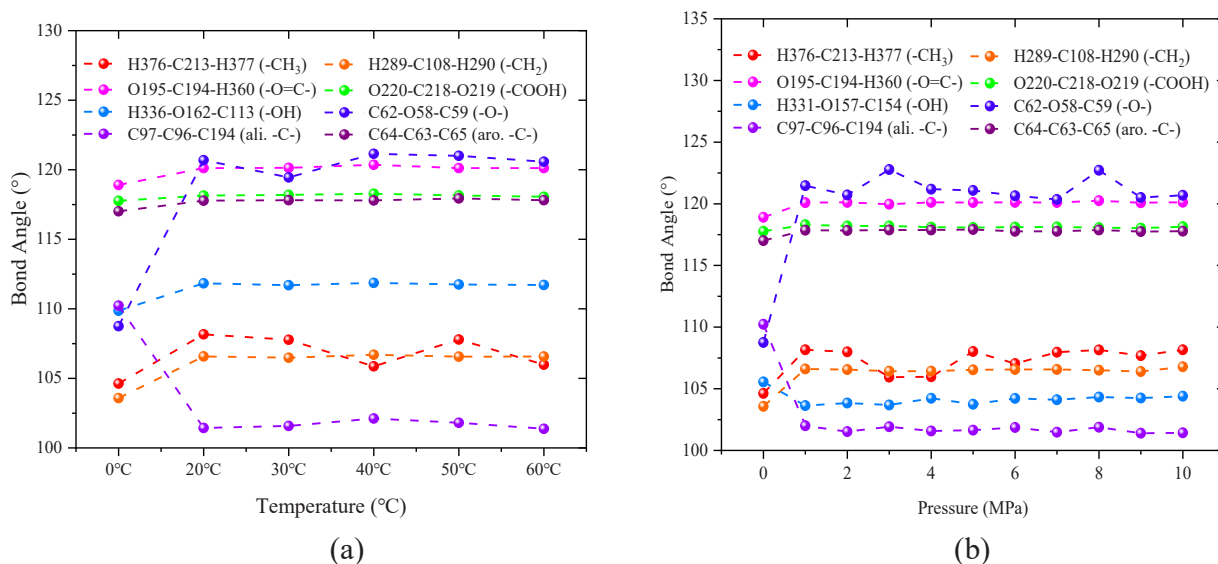
Fig. 9. Variation values of bond angles for different types of chemical structures. (a. Changes in bond length at different temperatures; b. Changes in bond length at different pressures.).

$101.89° - 109.76°$, $111.68° - 121.16°$, $117.16° - 119.35°$, $100.97° - 114.66°$, $105.97° - 125.87°$, $100.23° - 135.22°$ and $105.02° - 125.62°$), the deformation degree range of C-H, C-O, C-C, and O-H chemical bonds in the coal 3D-molecule is 0.03%– 1.09%, 0.08%– 0.97%, 0.01%– 2.94%, and 0.04%– 0.65% respectively, and the deformation degree of H-C-H (-CH₃), H-C-H (-CH₂), O-C-H (-O═C-), H-O-C (-OH), C-O-C (-O-), C-C-C (aliphatic -C-) and C-C-C (aromatic -C-) chemical structures in the coal 3D-molecule is 0.01%– 3.38%, 0.07%– 3.71%, 0.02%– 1.13%, 0.18%– 2.89%, 0.18%– 12.89%, 0.10%– 8.04% and 0.11%– 0.79%,

respectively. It can be seen that the chemical structures are more sensitive to methane adsorption than chemical bonds and their bond angles are more likely to change. Note that the deformation degree of the C-O-C (-O-) and C-C-C (aliphatic -C-) chemical structures is more severe than other chemical structures during methane adsorption in the coal molecular structure. These are the most likely to undergo deformation leading to swelling.

From Fig. 8, it can be seen that the C111-H295, C85-H276 (connected to the aromatic ring), C37-O221 (connected to an aromatic ring),
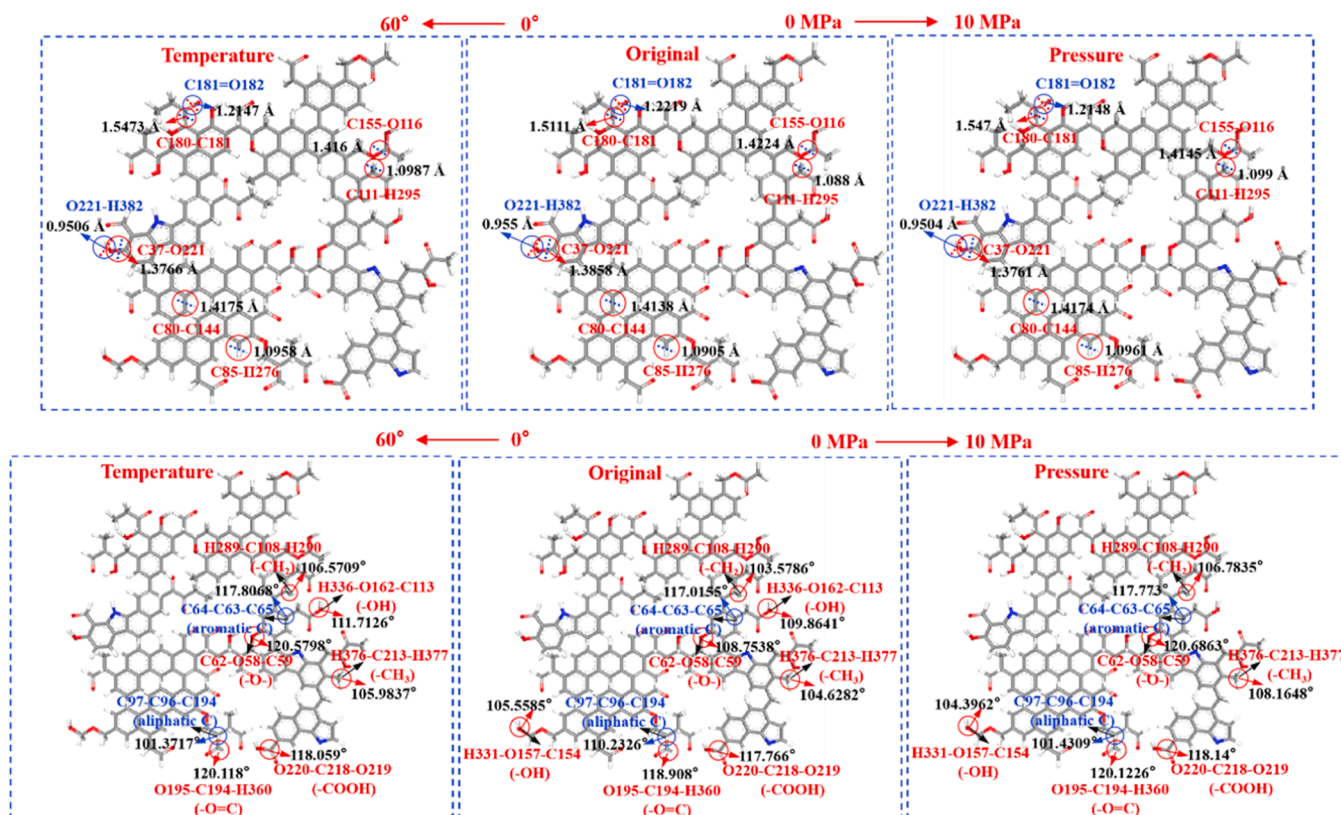

Fig. 10. Effect of adsorption of methane on the molecule conformation of different chemical bonds and different chemical structures.
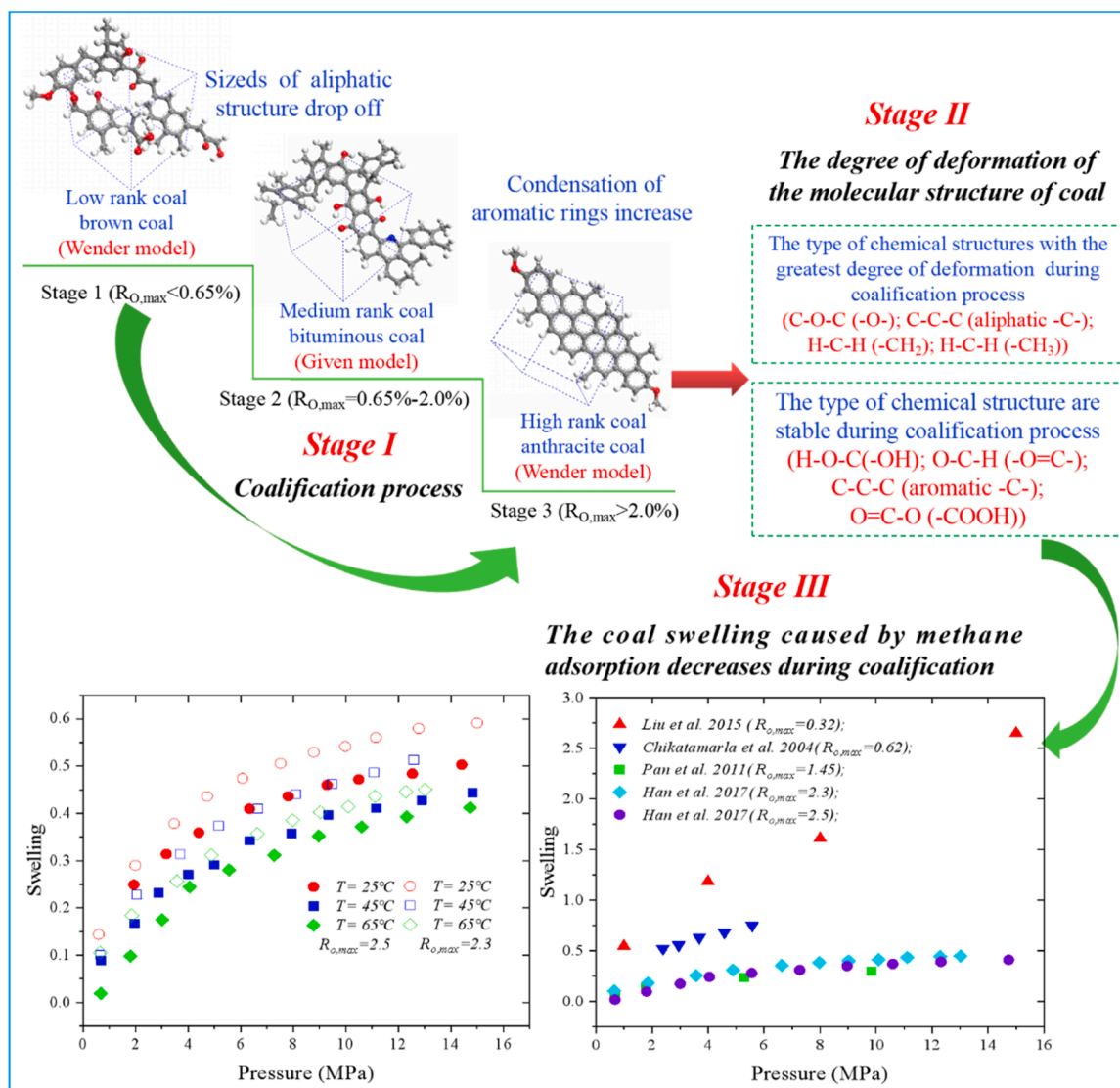
Fig. 11. Variations of methane-induced coal matrix swelling with coal rank. (The data and coal molecular model are from Given (1964), Wender (1976), Chikatamarla et al. (2004), Pan and Connell (2011), Liu et al. (2015), Han et al. (2017), respectively.).

C155-O166, C181 =O182, C180-C181, C80-C144 (aromatic ring), O221-H382 chemical bonds are the most variable in terms of bond length deformations among the C-H, C-O, C-C, and O-H chemical bond types. Simultaneously, it was found that the change in bond lengths is not obvious. From these results, it appears that the magnitudes of the deformations of bond types are in the order: C-C > C-H > C-O (connected to the aromatic ring) > C═O > C-O > C-H (connected to the aromatic ring) > O-H > C-C (aromatic ring) in the coal macromolecular structure. This result indicates that the chemical bonds connected to the aromatic rings are more stable than the aliphatic structures in the same type of bonds.

Based on the above discussions (Fig. 7), it appears that the absolute values of C-H, C-O, C-C, and O-H bond lengths are not significantly altered by the adsorption of methane. In contrast, it has been demonstrated that the adsorption of methane in the molecular structures of coal can induce changes in the bond angles of the different types of chemical structures (Fig. 9). From Fig. 9, it can be observed that the H376-C213-H377 (-CH$_3$), H289-C108-H290 (-CH$_2$), O195-C194-H360 (-O═C-), O220-C218-O219 (-COOH), H336-O162-C113 and H331-O162-C113 (-OH), C62-O58-C59 (-O-), C97-C96-C194 (aliphatic -C-), C64-C63-C65 (aromatic -C-) chemical structures are the most significantly affected by adsorption of methane. In addition, the spatial

locations of the bond angle deformations of methyl (-CH$_3$), methylene (-CH$_2$), carbonyl (-O═C-), carboxyl (-COOH), hydroxyl (-OH), ether (-O-), aliphatic carbon (aliphatic -C-) and aromatic carbon (aromatic -C-) functional bond types do not vary significantly with differences in temperature and pressure. In particular, bond angle changes are most pronounced in the methyl (-CH$_3$), methylene (-CH$_2$), ether (-O-), and aliphatic carbons structures. Compared with other chemical structures, aromatic carbon (aromatic -C-) chemical structures are stable, with no significant changes in bond angles. Consequently, it appears that the bond angles with the largest deformation are C-O-C (-O-) > C-C-C (aliphatic -C-) > H-C-H (-CH$_2$) > H-C-H (-CH$_3$) > H-O-C (-OH) > O-C-H (-O═C-) > C-C-C (aromatic -C-) > O═C-O (-COOH) in the coal macromolecular structure. This is consistent with the previous studies that the adsorption of methane has the greatest effects on the ether (-O-), aliphatic structure carbon (aliphatic -C-), methylene (-CH$_2$) and methyl (-CH$_3$) chemical structures in the coal 3D-molecule model.

4.4. Changes in coal molecular structure during methane adsorption

As demonstrated in the previous discussion, the adsorption of methane by the coal 3D macromolecular structure can induce changes in several different chemical structures. In contrast, the chemical bonds are

less prone to alter by methane adsorption than chemical structures. This can be seen in Fig. 10, in which the differences in the deformation of bond angles of different types of chemical structures as a function of temperature or pressure are shown. The deformation of the chemical molecular structures will cause the distortion and swelling of the coal volume, which will reduce the pore space and hinder the movement of methane molecules. In addition, the results show that the bond angles of ether (-O-), methyl (-CH$_3$) and methylene (-CH$_2$) chemical structures first increase and then decrease. In contrast, the bond angle of aliphatic carbon (-C-) decreases sharply and then increases or continues to decrease. After that, the change of the bond angles tends to a steady state (Fig. 9). While the chemical bonds are less prone to deformation, indicating that it is less affected during the adsorption of methane, and the same results can also be seen from the deformation degree of chemical bonds (Table 2, Table 3). In addition, methane absorption induces a deformation of the molecular structure of the coal, with the variation in surface potential energy being a factor that cannot be ignored. Based on the energy balance approach, Pan and Connell (2007) assumed that the surface energy change caused by adsorption is equal to the elastic energy change of the coal solid. They noted that under high pressure conditions, the change in surface potential energy caused by adsorption is less than the work done by the bulk gas. Therefore, the coal swelling ratio induced by methane adsorption may decrease after a swelling maximum is reached. And the swelling ratio is closely related to the adsorption capacity of the coal.

Fig. 11 demonstrates that the swelling of the coal volume decreases with increasing vitrinite reflectance values (coal rank). In other words, as the degree of coal metamorphism increases, the methane adsorption-induced swelling will decrease the pore volumes of the coal matrix. The reason may be due to the thermal cleavage of aliphatic side chains in the molecular structure of the coal during increasing maturation and coalification. Simultaneously, the aromatic ring structures become more condensed (including the formation of fused ring structures), and the molecular structure of the coal is more stable (Mathews and Chaffee, 2012; Zhou et al., 2022). It can also be seen that as the pressure increases, the methane adsorption-induced coal swelling will increase. In contrast, as the temperature increases, methane adsorption-induced coal swelling will decrease. This result may be due to variations in the amount of methane and the surface potential energy of the coal (Pan and Connell, 2007). In addition, according to the deformation of different types of chemical structures, it is obvious that the deformation of the aliphatic structures is greater than that of the aromatic structures. With increasing coalification, the concentrations of aliphatic structures decrease and the aromatic structures become more condensed in the molecular structure of the coal. Consequently, the trend of methane adsorption-induced coal swelling is as follows: low rank coal > medium rank coal > high rank coal. And the permeability of coal also decreases with increasing coal maturity (Liu et al., 2018a, 2018b). This phenomenon clearly explains the methane adsorption induced-swelling at the molecular level. It is also responsible for the deformation of the molecular structure of different chemical structures in the coal 3D-molecule.

5. Conclusion

1. Changes in bond lengths during methane adsorption are small for the different types of chemical bonds. The largest deformation degrees occur in chemical bonds C-C, which is 0.01%– 2.94%. And the C180-C181 chemical bond in the aliphatic structure is more deformed than other types of bonds. Consequently, it appears that the altering of bond lengths is not a significant factor in coal swelling.

2. Bond angles are significantly more deformed than bond lengths. Compared with other chemical structures, the molecular structure of ether (-O-), aliphatic carbon (-C-), methylene (-CH$_2$) and methyl (-CH$_3$) chemical structures will be the most significantly altered by methane adsorption, which deformation degrees are 0.18%– 12.89%, 0.10%–

8.04%, 0.07%– 3.71%, 0.01%– 3.38%, respectively. And the largest deformation degrees occur in chemical structures C-O-C (-O-), and the C62-O58-C59 chemical structure is more deformed than the other types of chemical structures.

3. In the coal 3D-macromolecular structure, the bonds connected to the aromatic ring are more stable than those in aliphatic structures. And the methane adsorption-induced coal swelling is mainly caused by altering bond angles of different chemical structures.

CRediT authorship contribution statement

Zhen Shen: Writing - original draft, Experiments, Simulation, Conceptualization. **Yu Liu:** Conceptualization, Resources (Samples), Writing - review & editing. **Junhuan Lei:** Simulation guidance, Processing data. **Weijun Shen:** Writing guidance. **Yuheng Wang:** Simulation guidance, Processing data. **Cheng Xu:** Collection of simulated data. **Jiaxun Gong:** Collection of simulated data;.

Declaration of Competing Interest

The authors declare that they have no known competing financial interests or personal relationships that could have appeared to influence the work reported in this paper.

Acknowledgments

References

Chen, L., Wang, L., Yang, T., Yang, H., 2021. Deformation and swelling of coal induced from competitive adsorption of CH$_4$/CO$_2$/N$_2$. Fuel 286, 119356.

Chikatamarla, L., Cui, X., Bustin, R.M., 2004. Implications of volumetric swelling/shrinkage of coal in sequestration of acid gases. International Coalbed Methane Symposium Proceedings, Tuscaloosa, Alabama, 0435.

Day, S., Fry, R., Sakurovs, R., 2008. Swelling of Australian coals in supercritical CO$_2$. Int. J. Coal Geol. 74 (1), 41–52.

Given P.H., 1964. The chemical study of coal macerals. Advances in Organic Geochemistry: Proceedings of the International Meeting in Milan 1962, 39–48.

Gotzias, A., Tylianakis, E., Froudakis, G., Steriotis, T., 2013. Effect of surface functionalities on gas adsorption in microporous carbons: a Grand Canonical Monte Carlo study. Adsorption 19, 745–756.

Han, F., Chen, G., Liu, Z., Yang, J., 2017. Correlation of swelling and sorption properties of block coal sample. Fuel 188, 452–461.

Hu, H., Li, X., Fang, Z., Wei, N., Li, Q., 2010. Small-molecule gas sorption and diffusion in coal: Molecular simulation. Energy 35 (7), 2939–2944.

Levine, J.R., Gayer, R., Harris, I., 1996. Model study of the influence of matrix shrinkage on absolute permeability of coal bed reservoirs. Geol. Soc. Lond. Spec. Publ. 109 (1), 197–212.

Lin, J., Ren, T., Cheng, Y., Nemcik, J., 2021. Laboratory quantification of coal permeability reduction effect during carbon dioxide injection process. Process Saf. Environ. 148, 638–649.

Liu, J., Peach, C.J., Zhou, H., Spiers, C.J., 2015. Thermodynamic models for swelling of unconfined coal due to adsorption of mixed gases. Fuel 157, 151–161.

Liu, P., Nie, B., Zhao, Z., Zhao, Y., Li, Q., 2023. Characterization of ultrasonic induced damage on multi-scale pore/fracture in coal using gas sorption and μ-CT 3D reconstruction. Fuel 332, 126178.

Liu, S., Harpalani, S., 2013. A new theoretical approach to model sorption-induced coal shrinkage or swelling. AAPG Bull. 97 (7), 1033–1049.

Liu, Y., Zhu, Y., Li, W., Xiang, J., Wang, Y., Li, J., Zeng, F., 2016. Molecular simulation of methane adsorption in shale based on grand canonical Monte Carlo method and pore size distribution. J. Nat. Gas. Sci. Eng. 30, 119–126.

Liu, Y., Zhu, Y., Liu, S., Li, W., Tang, X., 2018. Temperature effect on gas adsorption capacity in different sized pores of coal: experiment and numerical modeling. J. Petrol. Sci. Eng. 165, 821–830.

Liu, Y., Zhang, C., Zhang, Y., 2021. Evolution mechanism of methane adsorption capacity in vitrinite-rich coal during coalification. J. Nat. Gas. Sci. Eng. 96, 104307.

Liu, Z., Liu, D., Cai, Y., Pan, Z., 2018. The impacts of flow velocity on permeability and porosity of coals by core flooding and nuclear magnetic resonance: Implications for coalbed methane production. J. Petrol. Sci. Eng. 171, 938–950.

Majewska, Z., Majewski, S., Ziętek, J., 2010. Swelling of coal induced by cyclic sorption/desorption of gas: experimental observations indicating changes in coal structure due to sorption of CO$_2$ and CH$_4$. Int. J. Coal Geol. 83 (4), 475–483.

Mathews, J.P., Chaffee, A.L., 2012. The molecular representations of coal-a review. Fuel 96, 1–14.

Meng, Q., Wang, L., Yang, D., Xing, J., 2022. Methane and helium adsorption of coal and its related deformation under different temperature and pressures. Energy Source Part A 44 (2), 3929–3944.

Meng, Y., Li, Z., 2017. Triaxial experiments on adsorption deformation and permeability of different sorbing gases in anthracite coal. J. Nat. Gas. Sci. Eng. 46, 59–70.

Moffat, D.H., Weale, K.E., 1955. Sorption by coal of methane at high pressure. Fuel 34, 449–462.

Moore, T.A., 2012. Coalbed methane: a review. Int. J. Coal Geol. 101, 36–81.

Mosher, K., He, J., Liu, Y., Rupp, E., Wilcox, J., 2013. Molecular simulation of methane adsorption in micro- and mesoporous carbons with applications to coal and gas shale systems. Int. J. Coal Geol. 109–110, 36–44.

Palmer, I., Mansoori, J., 1998. How permeability depends on stress and pore pressure in coalbeds: a new model. SPE Reserv. Eval. Eng. SPE 52607, 539–544.

Pan, Z., Connell, L.D., 2007. A theoretical model for gas adsorption-induced coal swelling. Int. J. Coal Geol. 69 (4), 243–252.

Pan, Z., Connell, L.D., 2011. Modelling of anisotropic coal swelling and its impact on permeability behavior for primary and enhanced coalbed methane recovery. Int. J. Coal Geol. 85 (3–4), 257–267.

Pan, Z., Wood, D.A., 2015. Coalbed methane (CBM) exploration, reservoir characterization, production, and modelling: a collecting of published research (2009-2015). J. Nat. Gas. Sci. Eng. 26, 1472–1484.

Pan, Z., Connell, L.D., Camilleri, M., 2010a. Laboratory characterization of coal permeability for primary and enhanced coalbed methane recovery. Int. J. Coal Geol. 82, 252–261.

Pan, Z., Connell, L.D., Camilleri, M., Connelly, L., 2010b. Effects of matrix moisture on gas diffusion and fluid flow in coal. Fuel 89, 3207–3217.

Robertson, E.P., Christiansen, R.L., 2005. Measurement of sorption induced strain. International Coalbed Methane Symposium, Tuscaloosa, Alabama, 0532.

Shen, Z., Meng, Z., 2022. Enhancing the efficiency of coal bed methane recovery by injecting carbon dioxide based on an anthracite coal macromolecular model and simulation methods. Energy Fuels 36 (12), 6329–6342.

St. George, J.D., Barakat, M.A., 2001. The change in effective stress associated with shrinkage from gas desorption in coal. Int. J. Coal Geol. 69, 83–115.

Sun, H., 1998. COMPASS: an ab initio force-field optimized for condensed-phase applications overview with details on alkane and benzene compounds. J. Phys. Chem. B 102, 7338–7364.

Vandamme, M., Brochard, L., Lecampion, B., Coussy, O., 2010. Adsorption and strain: the CO_2- induced swelling of coal. J. Mech. Phys. Solids 58 (10), 1489–1505.

Wang, R., Wang, Q., Niu, Q., Pan, J., Wang, H., Wang, Z., 2020. CO_2 adsorption and swelling of coal under constrained conditions and their stage-change relationship. J. Nat. Gas. Sci. Eng. 76, 103205.

Wang, X., Cheng, Y., Zhang, D., Yang, H., Zhou, X., Jiang, Z., 2021. Experimental study on methane adsorption and time-dependent dynamic diffusion coefficient of intact and tectonic coals: implications for CO_2-enhanced coalbed methane projects. Process Saf. Environ. 156, 568–580.

Wang, Z., Fu, X., Pan, J., Deng, Z., 2023. Effect of N_2/CO_2 injection and alternate injection on volume swelling/ shrinkage strain of coal. Energy (275), 127377.

Wender, I., 1976. Catalytic synthesis of chemicals from coal. Catal. Rev. -Sci. Eng. 14 (1), 97–129.

Zhang, H., Diao, R., Chan, H., Mostofi, M., Evans, B., 2020. Molecular simulation of the adsorption-induced deformation during CO_2 sequestration in shale and coal carbon slit pores. Fuel 272, 117693.

Zhang, J., Liu, K., Clennell, M.B., Dewhurst, D.N., Pervukhina, M., 2015. Molecular simulation of CO_2–CH_4 competitive adsorption and induced coal swelling. Fuel 160, 309–317.

Zhang, Q., Liu, X., Nie, B., Wu, W., Wang, R., 2022. Methane sorption behavior on tectonic coal under the influence of moisture. Fuel 327, 125150.

Zhou, B., Yang, S., Jiang, X., Cai, J., Xu, Q., Song, W., Zhou, Q., 2022. The reaction of free radicals and functional groups during coal oxidation at low temperature under different oxygen concentrations. Process Saf. Environ. 150, 148–156.